MESOSCALE ANALYSIS OF A CAROLINA COASTAL FRONT

SETHU RAMAN, NEERAJA C. REDDY and DEVDUTTA S. NIYOGI
State Climate Research Laboratory, Department of Marine, Earth and Atmospheric Sciences, North Carolina State University, Raleigh, NC 27695-8208, U.S.A.

(Received in final form 17 June, 1997)

Abstract. During the Intensive Observation Period (IOP) 7 (22 February 1986) of the Genesis of Atlantic Lows Experiment a persistent coastal front was observed along the Carolina coast in the eastern United States. An intensive baroclinic zone, associated with the cold air damming to the east of the Appalachian Mountains, and the warm marine atmospheric boundary layer over the Gulf Stream, resulted in a northeasterly low-level geostrophic wind maximum near the coast.

Two convergence zones were observed, one near the shore and the other near the western edge of the Gulf Stream. The convergence zone near the coastline was relatively weaker than that near the Gulf Stream. The differential surface thermal forcing caused enhanced convergence associated with the frontogenesis, and a meso-low was observed over the offshore front. The terms in the frontogenesis equation are estimated, and the diabatic term is found to be larger than the frontogenetic confluence term along the shore.

Key words: GALE, Coastal front, Atmospheric boundary layer, Gulf Stream, Mesoscale analysis, North Carolina

1. Introduction

Strong thermal gradients occur during winters off the coast of the Carolinas (eastern U.S.) due to the presence of the Gulf Stream with sea-surface temperatures (SSTs) of about 298 K. The adjacent coastal waters, on the other hand, have SSTs typically in the range of 279 K to 282 K and the land has surface temperatures varying from 273 K to 283 K depending on the time of the day. Such large horizontal variations in the surface temperatures cause sharp gradients in the surface turbulent heat fluxes. These strong gradients in heat fluxes enhance mesoscale circulation and the associated convergence. One such mesoscale convergence usually observed during winters in this region is the Carolina coastal front. Since these fronts are surface induced, they are shallow with a typical height less than 1000 m.

The importance of the Gulf Stream heating in the evolution of these coastal fronts has been studied by several investigators (Bosart, 1975; Riordan, 1990; Holt and Raman, 1990, 1992; Huang and Raman, 1990, 1992; Doyle and Warner, 1990, 1993). Other process that occur during coastal frontogenesis are cold air damming along the Appalachian Mountains (Richwein, 1980), convective rainbands along the Gulf Stream (Huang and Raman, 1992) and low-level jets (Doyle and Warner, 1993).

The purpose of this paper is to document the mean structure of the marine boundary layer during a coastal frontogenesis and the development of a meso-low observed offshore of the coast of Carolinas on 22 February 1986. For the present

Boundary-Layer Meteorology **86:** 125–145, 1998.

study, observations collected during GALE IOP#7 (February 21 and 22, 1986) are used. The primary objective is to understand the interaction between the dynamics of the coastal front and the underlying SST discontinuity. The other objective of this paper is to present boundary-layer observations of mesoscale circulation associated with the Gulf Stream during the formation of the coastal front.

2. Observations

Observations made during GALE have been discussed in detail by Mercer and Kreitzberg (1986), Dirks et al. (1988) and Raman and Riordan (1988). A variety of National Weather Service and GALE surface and upper-air data are used in this study. Observations made with the National Center for Atmospheric Research (NCAR) King Air research aircraft on 22 February 1996 will be examined to study the mesoscale circulation over the Gulf Stream. Aircraft data will be the primary dataset, but supporting observations from special surface data, and vertical soundings using Cross Chain Loran Atmospheric Sounding Systems (CLASS), miniradiosondes, special National Weather Service (NWS) rawinsondes and Omega dropwindsondes will also be used. The special GALE surface data were obtained from 51 Portable Automated Mesonet (PAM) II sites, eight instrumented GALE research buoys, National Oceanic and Atmospheric Administration (NOAA) buoys and platforms and one research vessel, R/V Cape Hatteras.

The flight track of the NCAR King Air aircraft on 22 February offshore of Carolinas is given in Figure 1 along with the high resolution (1.1 km) sea surface temperature (SST) analysis of 19 February 1986. Due to the presence of clouds on 22 February, the SST analysis on 19 February (the closest date on which the cloud activity was less offshore) has been used. The SST data were obtained from the NOAA-9 satellite.

Near-shore waters were cold, especially north of Cape Hatteras and along the coast. A strong baroclinic zone exists off the Carolinas. An oceanic feature called a filament, which is a tongue-like extrusion of the Gulf Stream warm waters into the cold shelf waters was aligned almost parallel to the east coast at about 60–70 km from the shore. The length and the width of this filament were about 200 km and 50 km, respectively. A strong oceanic thermal gradient, generally known as the mid-shelf front (located at D) also existed as shown in Figure 1. Reddy and Raman (1994) showed that a meso-low developed over a Gulf Stream filament on 10 February 1986 and later intensified into a mid-latitude cyclone on 11 February 1986.

The initial flight plans of the King Air on 22 February were to obtain flux profiles over the mid-shelf front and the Gulf Stream core during a period of southwesterly flow and to investigate the coastal front structure. The King Air flight took a level wing descent at B (33.5° N, 77.8° W) from 3000 m over the cold shelf waters (SSTs around 284 K) at 1745 UTC on 22 February (Figure 2). Then the flight proceeded

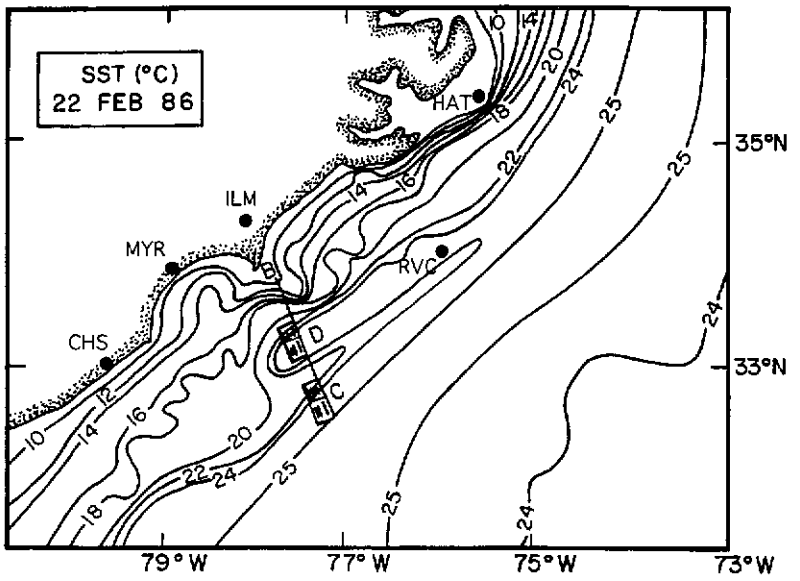

Figure 1. Flight tracks of the King Air aircraft on 22 February. The contours indicate the sea surface temperatures (in °C). RVC indicates the location of Research Vessel Cape Hatteras. Locations of Cape Hatteras (HAT), Wilmington (ILM), Myrtle Beach (MYR) and Charleston (CHS) are shown in the figure.

from B to C (32.8° N, 77.4° W) at 40 m altitude. This low level transect was about 160 km long (Figure 1). A vertical stack consisting of a series of level 300–400 sec legs (23.1–31 km in length at an aircraft speed of 77 m s^{-1}) at six altitudes (30 m, 100 m, 150 m, 250 m, 350 m and 1100 m) was flown. Another low-level transect was made by the King Air from C to D at 40 m altitude. A vertical stack consisting of a series of level 300 s to 400 s flights at four altitudes (40 m, 300 m, 150 m, 1000 m) was flown at 1900 UTC at this location. A level wing ascent from 150 m to 2000 m was made at D at approximately 1930 UTC.

3. Instrumentation

Instrumentation on the aircraft used during GALE is discussed in detail by LeMone and Pennell (1980) and Lenschow and Spyers-Duran (1986). Only a brief discussion of the primary aircraft mean and turbulent data and analysis used in this study is included here. Both low-rate (1 Hz) and high-rate (20 Hz) data were obtained from the aircraft instrumentation system.

Ambient temperature was measured by a Rosemount temperature probe, dewpoint by an EG&G dewpoint hygrometer and pressure by a Rosemount pressure transducer. A gust probe with pressure ports on the nose of the King Air was used for sensing air motion. Both mean horizontal wind and turbulent fluctuations of the

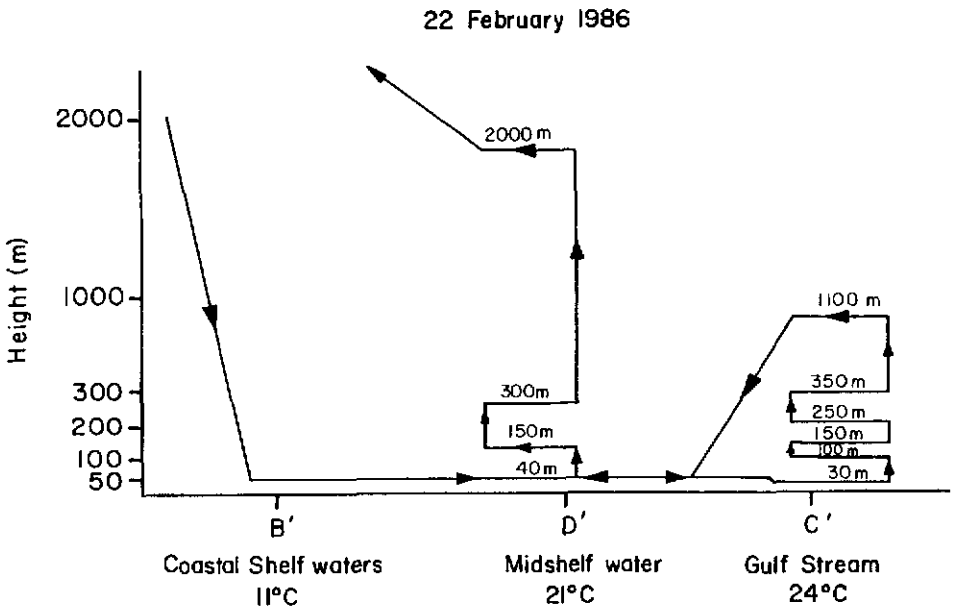

Figure 2. Vertical cross section of the aircraft flight track on 22 February 1986.

three air velocity components were obtained from the gust probe and the inertial navigation system (Brown et al., 1983). Calibration of the 20 Hz Lyman-α humidity data used the method of Lind and Shaw (1990) in which a linear regression of Lyman-α data on 1 Hz hygrometer data was performed. Values of SST were determined from the downward-viewing radiometer.

Mean and turbulence values over the length of each flight leg were then detrended by linear regression. Any spurious spikes, represented by values exceeding three standard deviations were removed. Means, standard deviations and fluxes were then computed from detrended data for each leg. Turbulence fluxes were calculated using simple statistics involving the covariance and correlation between the two variables of interest.

4. Synoptic Analysis

The synoptic conditions on 22 February 1986 were favorable for coastal frontogenesis offshore of the Carolinas. The 1200 UTC National Center for Environmental Prediction (NCEP) surface analysis is shown in Figure 3. The NCEP surface analysis positioned the surface cyclone (1010 mb) on the Georgia border with a strong cold front. This stationary front was along the South Carolina-Georgia border. A cold dome anticyclone of 1030 mb was located over James Bay (49.5° N, 77° W) well north of the GALE area. The presence of the cold anticyclone to the north

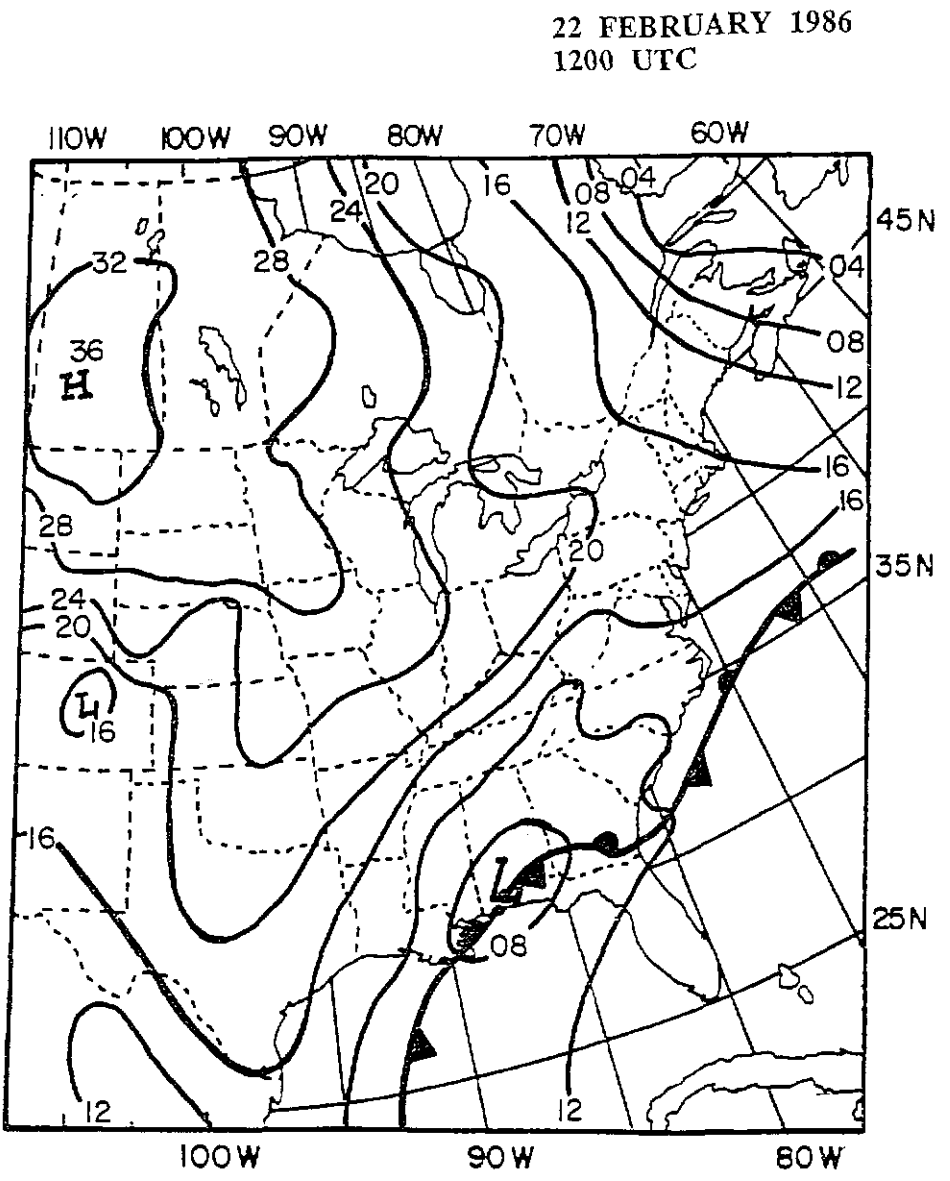

Figure 3. NCEP surface pressure analysis for 1200 UTC on 22 February 1986.

provided north-northeasterly flow along the coast at 1200 UTC (Figure 3) which is generally conducive for coastal frontogenesis (Bosart et al., 1972).

In the study region, the wind direction changed from northerly to easterly at 1800 UTC as the anticyclone moved eastward. Over land, however, the wind direction remained northeasterly as a smaller scale ridge of high pressure extended southwestward. This feature is commonly associated with cold air damming along the

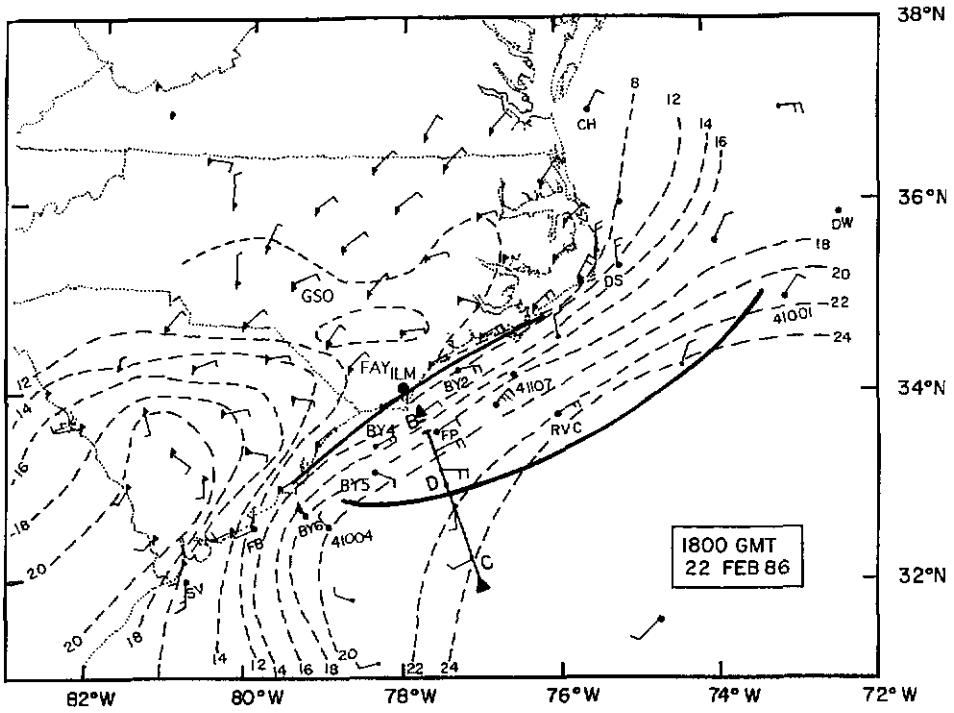

Figure 4. Surface mesoscale analysis of isotherms (°C) at 1800 UTC on 22 February 1986. Solid lines indicate the regions of low level convergence, one along the coastline and the other along the western edge of the Gulf Stream. BDC is the aircraft flight track: BY2, BY4, BY5 and BY6 are NCSU toroid buoys. 41001, 41004 and 41007 are NOAA buoys. RVC is Research Vessel Cape Hatteras. SV is Savannah Platform, CH is Chesapeake Bight Tower, DS, Diamond Shoals Light Tower. Greensboro (GSO) and Fayetteville (FAY) are the locations of upper air soundings.

east coast (Richwein, 1980). Such damming east of the Appalachians is considered important in subsequent coastal front formation (Bosart, 1975; Bosart et al., 1972; and Ballentine, 1980). Thus, a coastal frontogenesis was expected in this case.

5. Mesoscale Analysis

Mesoscale surface analysis from the PAM network, ships, and buoys for 0600–2300 UTC on 22 February in the region of the offshore coastal front is shown in Figure 4. At 06 UTC on 22 February, moderate northeasterly flow (5 m s^{-1}) occurred along the coast from Cape Hatteras (33.3° N; 75.5° W) to Wilmington. This was in contrast to the south-southwesterly flow in the vicinity of Charleston, SC (32.9° N, 80° W). Visible satellite imagery at 06 UTC (not shown) however, indicated little organized cloud activity in this region. Similar conditions prevailed up to 1200 UTC.

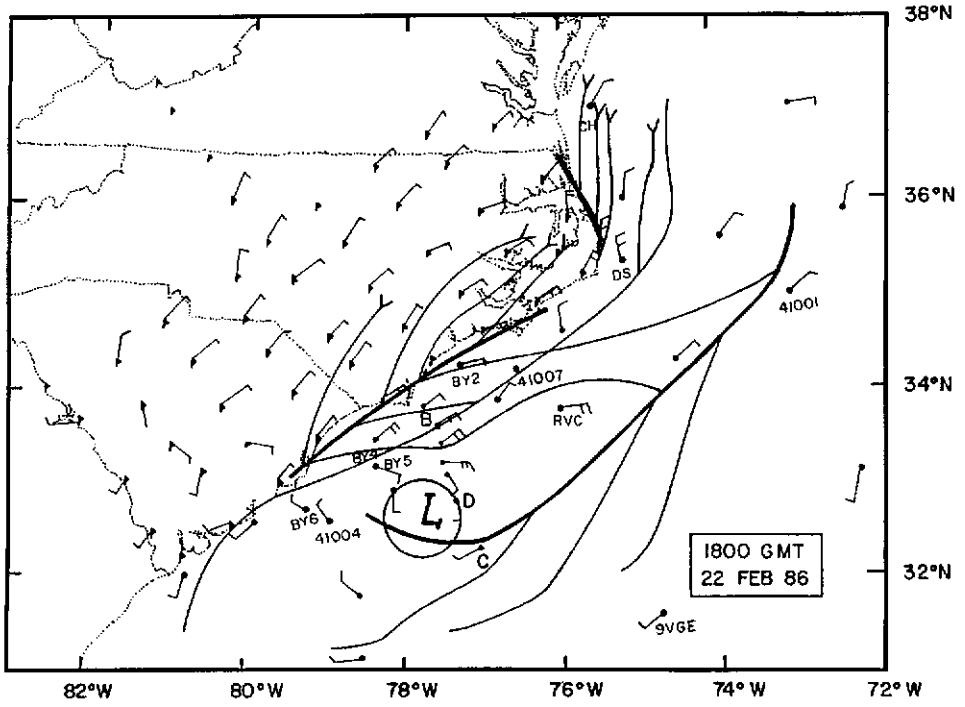

Figure 5. Surface mesoscale analysis of streamlines. Heavy solid lines indicate the confluence zones, one near the coast somewhat discontinuous and the other along the western edge of the Gulf Stream. The observation locations are as in Figure 4. A meso-low is located offshore.

For the mesoscale analysis at 1800 UTC (Figure 4), King Air aircraft data have been used. The line connecting B, D and C indicates the aircraft low level transect at approximately 1800 UTC. An interesting feature in the 1800 UTC satellite observations was the presence of organized cloud activity along the coastal front (not shown). Streamline analysis (Figure 5) indicates the development of a cyclonic rotation between 1700 UTC and 2100 UTC offshore (32.8° N, 77.5° W), indicating the development of a surface meso-low. The location of this cyclone was near the western edge of the Gulf Stream in the region of the NCAR King Air boundary-layer flight. When SSTs were superimposed on the mesoscale analysis (see Figure 1 and Figure 5), the location of the surface meso-low appeared to be over a Gulf Stream filament. Development of a meso-low offshore over a Gulf Stream filament on 10 February 1986 was documented by Reddy and Raman (1994). Geometry of these Gulf Stream filaments induce circulations favorable for the formation of meso-lows.

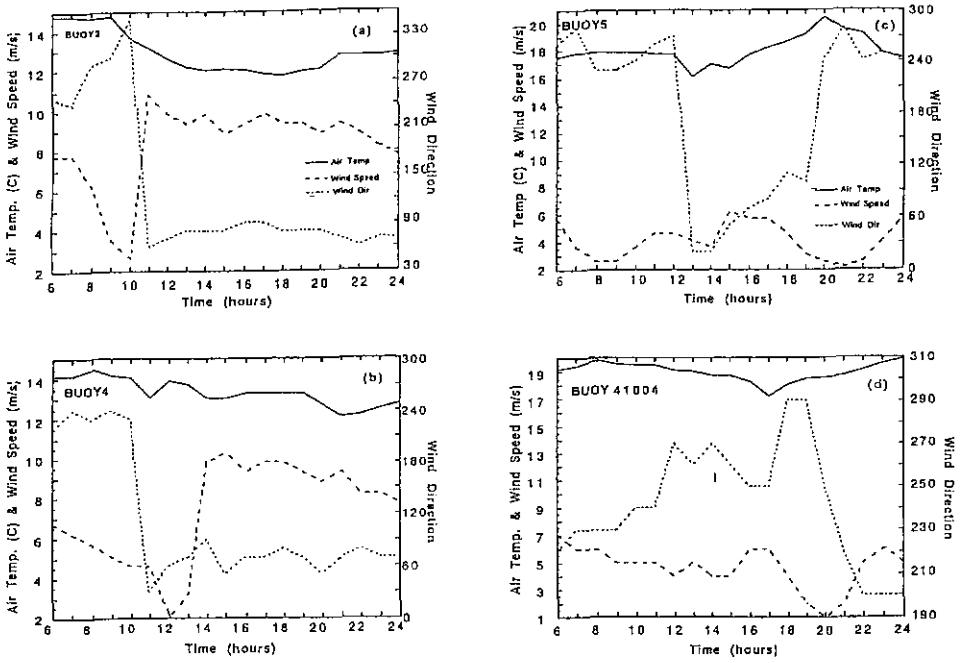

Figure 6. Time series of wind speed, wind direction and air temperature from 0600 UTC on 21 February to 0000 UTC 22 February at (a) Buoy 2, (b) Buoy 4, (c) Buoy 5, and (d) Buoy 41004 station.

6. Mesoscale Convergence and Circulation

As discussed before, the synoptic scale anticyclone centered over Canada at 1200 UTC on 22 February had moved sufficiently east to induce northerly or northeasterly flow along the east coast of the US. Cold continental air was well established over land with surface temperatures less than 281 K. In the vicinity of the Gulf Stream, however, SSTs were about 298 K (Figure 1). Thus a strong horizontal air temperature gradient was present offshore. These large surface temperature gradients in turn cause significant energy flux gradients in this region. Figure 6 illustrates the time history of air temperature, wind direction and wind speed measured at several marine sites (Buoy 2, Buoy 4, Buoy 5, RVC and NOAA Buoy 41004) starting from a time prior to the synoptic scale cold frontal passage and ending after the coastal front development. Locations of these marine sites are shown in Figure 1. Buoy 2 was in coastal shelf waters (283–285 K), Buoy 4 was in between the cold shelf and the midshelf waters, Buoy 5 and NOAA Buoy 41004 were in mid-shelf waters (291–293 K) and RVC was in warm Gulf Stream waters most of the time. However, the ship RVC was not stationary for the period 0000 UTC to 1200 UTC on 22 February.

Solid lines indicate the air temperatures, short dashed lines are wind direction and long dashed lines are wind speed variation. The coastal front location is apparent on these time series plots at various locations. As can be seen from Figure 6, the air temperature decreased as the front moved across. These changes in air temperatures are consistent with the changes in wind speed and wind direction. The coastal front passed Buoy 2 at 1000 UTC. At Buoy 4 located further offshore, the coastal front passed at 1200 UTC. At Buoy 5 and Buoy 41004 which were located in the midshelf waters, the coastal front passed at 1500–1700 UTC on 22 February. After the coastal frontal passage, the wind direction at these locations was primarily from land, in a southwesterly direction. Also, it is apparent from Figure 6 that stronger surface winds were present west of the frontal passage and weaker flow to the east. Similar variation in wind speed was found by Riordan (1990) for the 24 January 1986 coastal front case. The mesoscale analysis presented in Figure 4 also indicates that the strongest winds are found in a region where the largest thermal gradients are present.

Several investigators studying New England coastal fronts (Ballentine, 1980 and Nielsen, 1989) and east coast cyclogenesis (Hsu, 1984; Riordan, 1990; Holt and Raman, 1990, 1992; Huang and Raman, 1992; and Reddy and Raman, 1994) found evidence of sea-breeze-like direct thermal circulations, characteristic of the warm waters of the Gulf Stream. Similar circulation was observed on 22 February 1986 (Figures 4 and 6). Observations from the low level King Air aircraft taken at 40 m altitude from B (cold waters, SST = 283 K) to C (Gulf Stream waters, SST = 298 K) are shown in Figure 7. Spatial variations of SST, potential temperature, absolute humidity, wind speed, direction and vertical velocity are shown in Figure 7. This transect was taken from 1758 UTC to 1840 UTC (160 km long, with an aircraft speed of 77 m s^{-1}). SST variation showed a step-like increase towards the warm waters from 283 K over coastal waters to 293 K over the Gulf Stream. An expected increase in potential temperature and absolute humidity towards warmer Gulf Stream waters can be seen in Figures 7b and 7c, respectively. A horizontal temperature gradient (dT/dx) of 0.125K km^{-1} was estimated for this low level transect. There was an increase in the wind speed near the coastline and in the vicinity of the Gulf Stream with near-zero winds in between. Weak winds in this region could be due to the presence of a difluence zone between the two convergence regions associated with the coastal fronts discussed earlier. Noticeable change in wind direction near the western edge of the Gulf Stream was an indication of a low level circulation, in this case, the formation of a meso-low (Figure 7e). Vertical velocity fluctuations (Figure 7f) showed an increase in turbulence towards the Gulf Stream.

Figure 8 shows a cross section through the coastal front at 1800 UTC. Soundings at Greensboro, Fayetteville and Wilmington over land and King Air aircraft data at locations B, D and C over water were used. Solid lines show the potential temperature contours. The cross section of potential temperatures indicate packed isotherms. These strong temperature gradients identify the front. A near-neutral

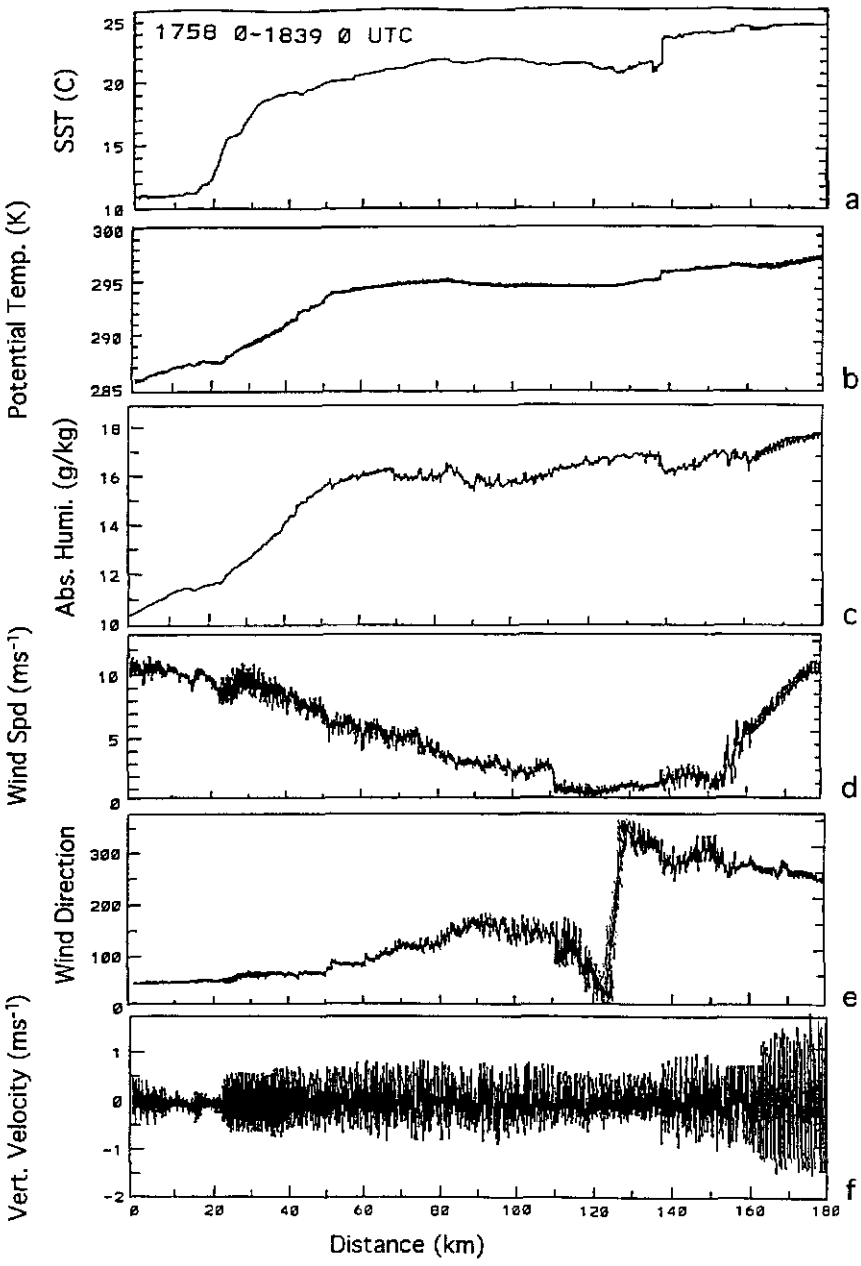

Figure 7. Low level transect by King Air aircraft from cold shelf waters to the Gulf Stream (a) SST, (b) potential temperature (K), (c) absolute humidity (g kg^{-1}), (d) wind speed (m s^{-1}), (e) wind direction, and (f) vertical velocity (m s^{-1}).

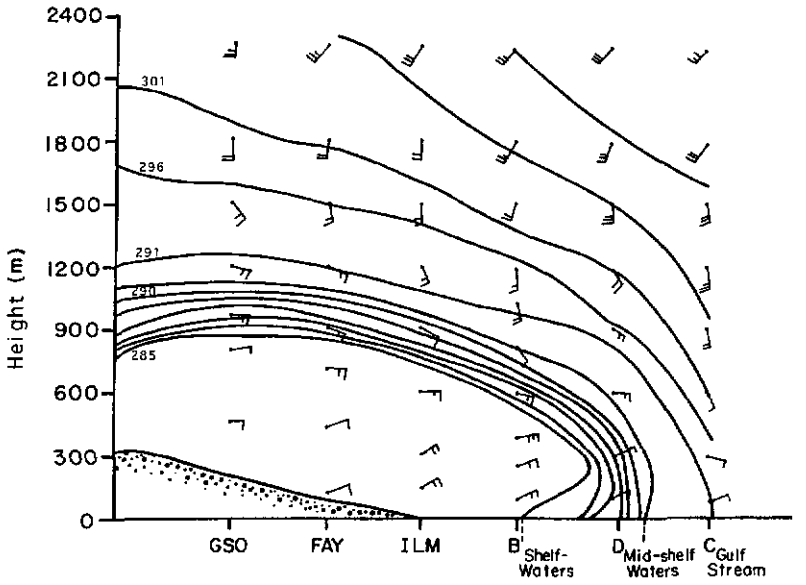

Figure 8. Cross section of the coastal front. Sounding data at Greensboro (GSO), Fayetteville (FAY) and Wilmington (ILM) and aircraft data at B, D and C are used in this analysis. See Figure 1 for their locations.

boundary layer existed in this frontal zone extending up to a height of about 500 m. Also, west of the coastal front a low-level jet was present. Significant change in wind direction across the front is clearly seen both in this vertical cross section as well as in the aircraft transect (shown in Figure 7). The front was located approximately over the mid shelf waters. The cross section of this coastal front is basically similar to that analyzed by Riordan (1990) for 24 January 1986.

Horizontal low-level convergence estimated from the buoy and aircraft data is shown in Figure 9. The contours of horizontal convergence on 22 February indicate convergence and divergence zones aligned parallel to the coast line (solid lines in Figure 9 are the centers of convergence zones). Mesoscale analysis shows a divergence zone along the shelf waters and convergence along the western edge of the Gulf Stream. Such convergence and divergence zones were also found during other intensive observation periods (IOP) of the GALE (Riordan, 1990; Holt and Raman, 1992; Reddy and Raman, 1994). At 1800 UTC, the estimated maximum divergence was about 4×10^{-4} s^{-1} and the maximum convergence 3.5×10^{-4} s^{-1}. Two distinctly separate flow regimes are apparent from the streamline analysis (Figure 5) and the estimated convergence. The first one is located over the shelf waters parallel to the coastline with a northeasterly wind. The other is located in the region of strong SST gradient (midshelf waters) with a stronger southwesterly wind. A cyclonic circulation developed in the vicinity of the Gulf Stream (see Figure 5). As discussed earlier, this circulation was over a Gulf Stream filament.

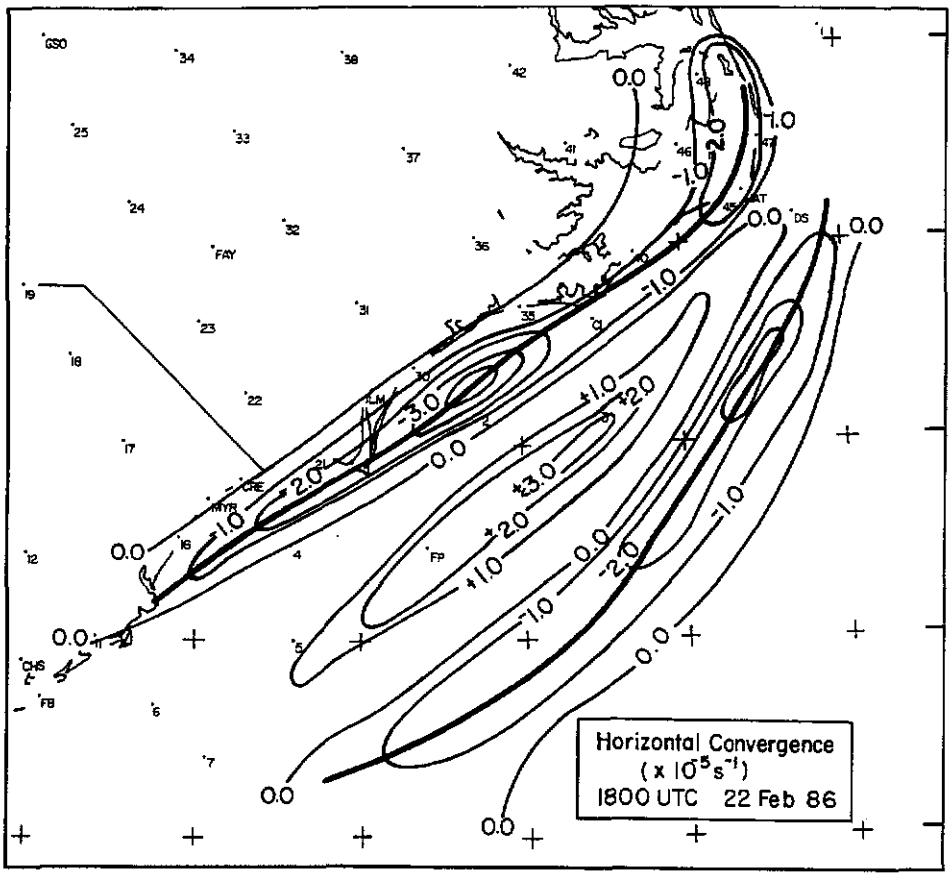

Figure 9. Spatial distribution of horizontal convergence (10^{-5} s^{-1}) at 1800 UTC on 22 February 1986.

7. Analysis of Frontogenesis

A frontogenetical function, as below, can be used to estimate the frontogenesis:

$$F = \frac{d}{dt}|\nabla\theta|$$

$$= \frac{1}{|\nabla\theta|}\left\{\frac{\partial\theta}{\partial x}\left[-\underset{1}{\frac{\partial u\partial\theta}{\partial x\partial x}}-\underset{2}{\frac{\partial v\partial\theta}{\partial x\partial y}}-\underset{3}{\frac{\partial w\partial\theta}{\partial x\partial z}}+\underset{4}{\frac{\partial}{\partial x}\left(\frac{\mathrm{d}\theta}{\mathrm{d}t}\right)}\right]\right.$$

$$\left.+\frac{\partial\theta}{\partial y}\left[-\underset{5}{\frac{\partial u\partial\theta}{\partial y\partial x}}-\underset{6}{\frac{\partial v\partial\theta}{\partial y\partial y}}-\underset{7}{\frac{\partial w\partial\theta}{\partial y\partial z}}+\underset{8}{\frac{\partial}{\partial y}\left(\frac{\mathrm{d}\theta}{\mathrm{d}t}\right)}\right]\right\} \tag{1}$$

where horizontal deformation or flow confluence are represented by terms 1, 2, 5 and 6, tilting effects by terms 3 and 7, and differential diabatic heating by

terms 4 and 8. By orienting the y-axis along the horizontal gradient of the potential temperature, and directing it towards the cold air, the rate of change in the horizontal temperature gradient can be expressed as:

$$\frac{\mathrm{d}}{\mathrm{d}t}\left(\frac{\partial\theta}{\partial y}\right) = \underset{1}{\frac{\partial w\partial\theta}{\partial y\partial z}} + \underset{2}{\frac{\partial v\partial\theta}{\partial y\partial y}} - \underset{3}{\frac{\partial}{\partial y}\left(\frac{\mathrm{d}\theta}{\mathrm{d}t}\right)}. \tag{2}$$

The first term on the right-hand side of Equation (2) is the tilting term. This term indicates the reorientation of the vertical gradient of potential temperature by differential vertical motions. In frontal zones, this is significant. However, near the surface in the frontal zones, the vertical motions are negligible. Thus, in the estimation of surface frontogenesis, this term can be neglected. The estimation of the other frontogenetic terms for the present case are based on the methodology adopted by Riordan (1990).

The second term on the right-hand side of Equation (2) is the confluence term. The spatial distribution of the confluence term is shown in Figure 10a. In estimating the confluence term, the wind field is considered only along the y-axis. Thus, this term is primarily the horizontal convergence directed normal to the front. The estimation of the confluence term involves the products of derivatives (Equation (2)). As the data coverage offshore was not homogeneous, transects were used to estimate this term. Contours of the confluence term were estimated from the five frontal transects (C1, C2, C3, C4 and C5). The maximum confluence is in the region of maximum horizontal convergence (Figure 10a).

The maximum confluence offshore at the Carolinas and Cape Hatteras is estimated to be about 2.65 K (100 km)$^{-1}$ h^{-1} and 4.25 K (100 km)$^{-1}$ h^{-1}, respectively. The estimated maximum frontogenesis from the observations during the 24 January 1986 coastal front was about 4 K (100 km)$^{-1}$ h^{-1} (Riordan, 1990; Doyle and Warner, 1990). The maximum values in the present case are slightly less as compared to those observed on 24 January 1986 coastal front and three times larger than that of the Presidents' Day Storm (Bosart and Lin, 1984). It is also about eight times smaller than the model predicted values of 24 January coastal front (Huang and Raman, 1992). Despite these differences in the numerical values, a close similarity exists in the flow patterns. The maximum flow confluence offshore of Wilmington and Hatteras are 2.15 K (100 km)$^{-1}$ h^{-1} and 2.85 K (100 km)$^{-1}$ h^{-1}, respectively. It appears from this analysis that the confluence term can be a dominating forcing in the coastal frontogenesis.

The last term in Equation (2) is the differential diabatic heating across the front. This term can be written as:

$$-\frac{\partial}{\partial y}\left[\underset{1}{\frac{\partial\theta}{\partial t}} + \underset{1}{u\frac{\partial\theta}{\partial x}} + \underset{2}{v\frac{\partial\theta}{\partial y}} + \underset{3}{w\frac{\partial\theta}{\partial z}}\right] = -\frac{\partial}{\partial y}\left[\underset{\mathrm{I}}{-\frac{\partial\overline{w'\theta'}}{\partial z}} - \underset{\mathrm{II}}{\frac{\partial R_n}{\partial z}} + \underset{\mathrm{III}}{L}\right]. \tag{3}$$

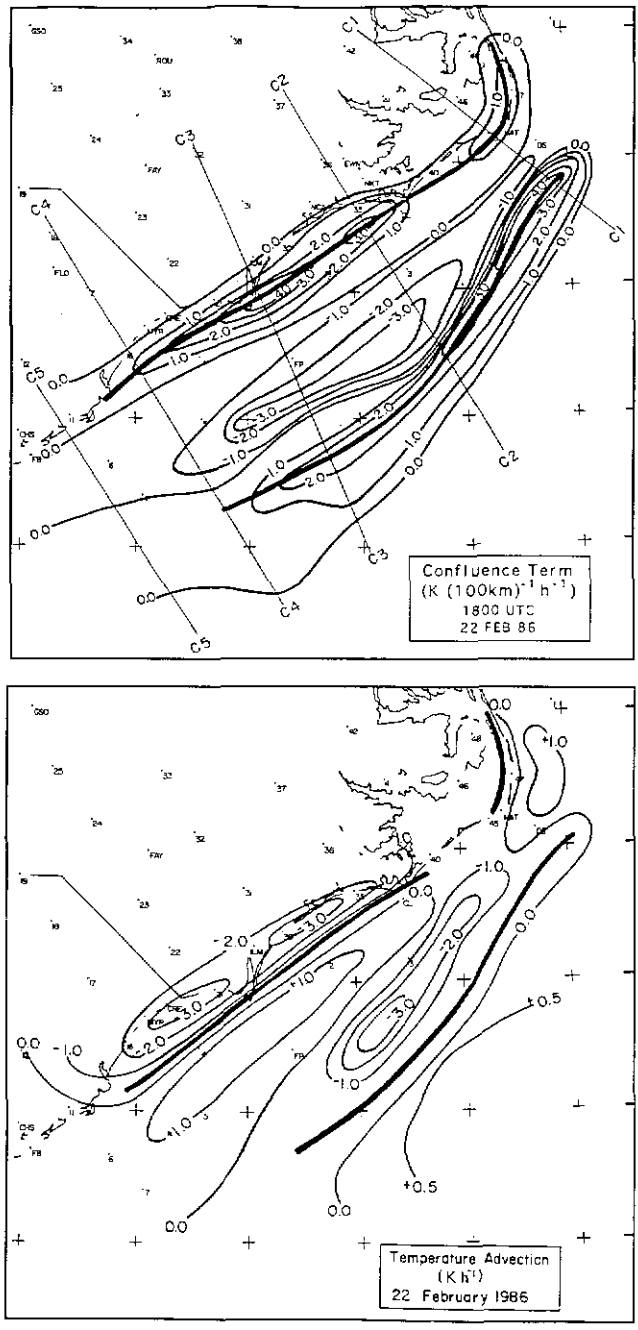

Figure 10. (a) Spatial distribution of the confluence term (K (100 km)$^{-1}$ h^{-1}) at 1800 UTC on 22 February 1986. Cross sections C1 to C5 provided observations from which the surface analysis was made. Numbers over land indicate the PAM stations. (b) Spatial distribution of temperature advection (K (100 km)$^{-1}$ h^{-1}) at 1800 UTC on 22 February 1986.

The terms on the left-hand side of the equation are local change of potential temperature and advection. Assuming that the vertical motions are negligible near the surface, the diabatic term can be estimated using the local change and horizontal advection of potential temperature. The terms on the right-hand side of Equation (3) are the divergence of the sensible heat flux, the divergence of the net radiative flux and the surface turbulent latent heat flux.

The spatial distribution of horizontal advection is shown in Figure 10b. Cold air advection from the northeast was prominent closely following the coastal front. The maximum cold air advection near the coast was -3.65 K (100 km)$^{-1}$ h^{-1}. Ahead of the front, weak warm air advection was present over the Gulf Stream, with a maximum value of 0.5 K (100 km)$^{-1}$ h^{-1}. This warm air advection was from the southwest.

As mentioned above, the other component which contributes to the diabatic term is the local change in temperature. The spatial distribution of local air temperature change is shown in Figure 11a. This term is difficult to estimate, especially offshore where the temporal and spatial distribution of measurements are sparse. These values are estimated following Riordan (1990). The local temperature change over land was estimated using data and Portable Automated Mesonet (PAM) data and was averaged over a 3-hour interval at 1800 UTC. The dots with numbers adjacent to them indicate locations of the PAM stations. Over water, these values were estimated by subtracting the air temperatures at 1500 UTC from the corresponding values at 2100 UTC. A weak warming existed along the coastline over the land surface with a maximum value of about 1.0 K (100 km)$^{-1}$ h^{-1}. This could be due to the expected warming of the land during daytime. Offshore, a weaker warming was apparent. This warming contributed to the heat flux divergence in this region.

The local rate of change (Figure 11a) and the advective component (Figure 10b) are combined and shown in Figure 11b. The net effect was to cool the air because of strong cold advection from northeast behind the front. The distribution of the diabatic heating term is shown in Figure 12a. Appreciable diabatic warming occurred near the front with estimated maximum values ranging from 6 to 7 K (100 km)$^{-1}$ h^{-1}. The maximum values were generally found over the regions of strong SST gradients. The diabatic heating term is somewhat weaker along the Carolina coastline. A value of 5 K (100 km)$^{-1}$ h^{-1} was reported by Riordan (1990) for the 24 January 1986 coastal front. The spatial distribution of total frontogenesis is shown in Figure 12b. The total contribution from the diabatic term and the confluence term is positive along the coastal front.

8. Mean Structures of the MBL and the Low Level Jet

Vertical variation of wind speed, wind direction, air temperature and absolute humidity at B (over cold waters) is shown in Figure 13. This vertical sounding was

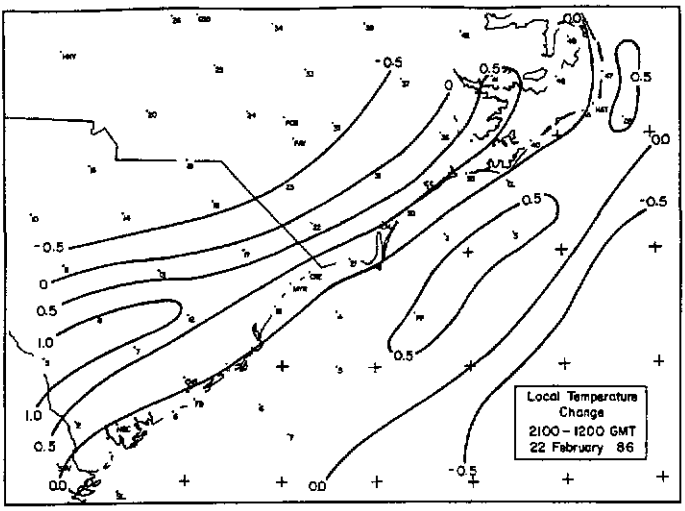

a

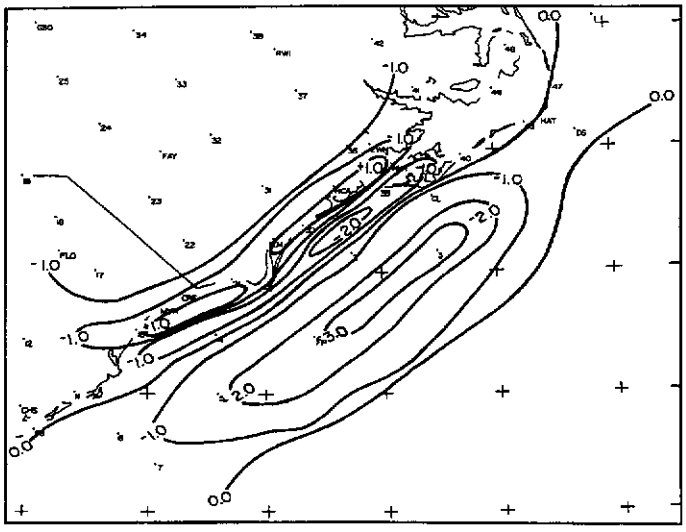

b

Figure 11. (a) Spatial distribution of local temperature change (K (100 km)$^{-1}$ h^{-1}) from 2100 UTC on 21 February 1986 to 1200 UTC on 22 February 1986. (b) Spatial distribution of the sum of temperature advection and local temperature change (K (100 km)$^{-1}$ h^{-1}) on 22 February 1986.

taken by the King Air aircraft from an altitude ranging from 30 m to 3000 m at 1746 UTC. The SST at this location (33.67° N, 77.75° W) was 285 K.

The potential temperature profile (Figure 13a) indicated the existence of a stable boundary layer up to 900 m and a neutral layer between 900 m and 1900 m. At this location, near surface air temperature (286 K) was higher than the underlying SST (285 K) for the northeasterly flow, forming a stable layer evident at location B. The neutral layer above the stable boundary layer was due to the advection of warm dry

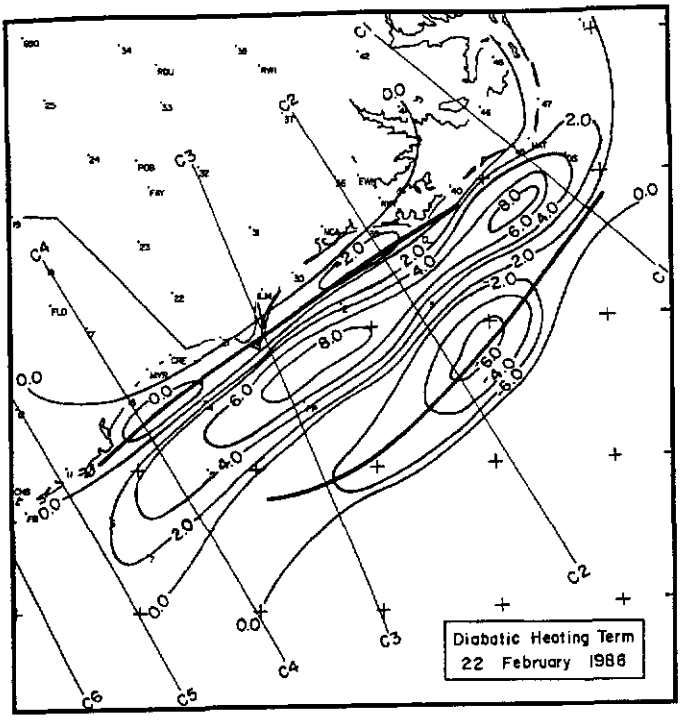

a

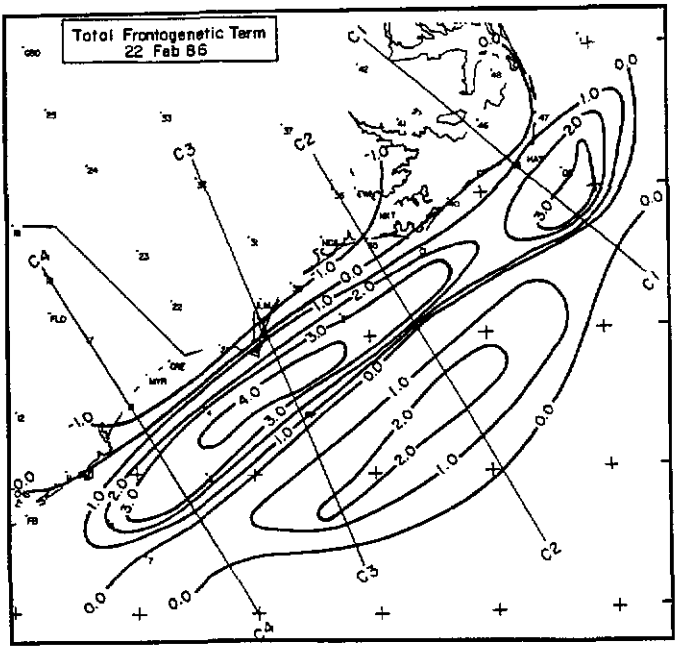

b

Figure 12. (a) Spatial distribution of the diabatic heating term (K (100 km)$^{-1}$ h^{-1}) on 22 February 1986 at 1800 UTC. (b) Spatial distribution of the total frontogenetic term (K (100 km)$^{-1}$ h^{-1}) on 22 February 1986 at 1800 UTC.

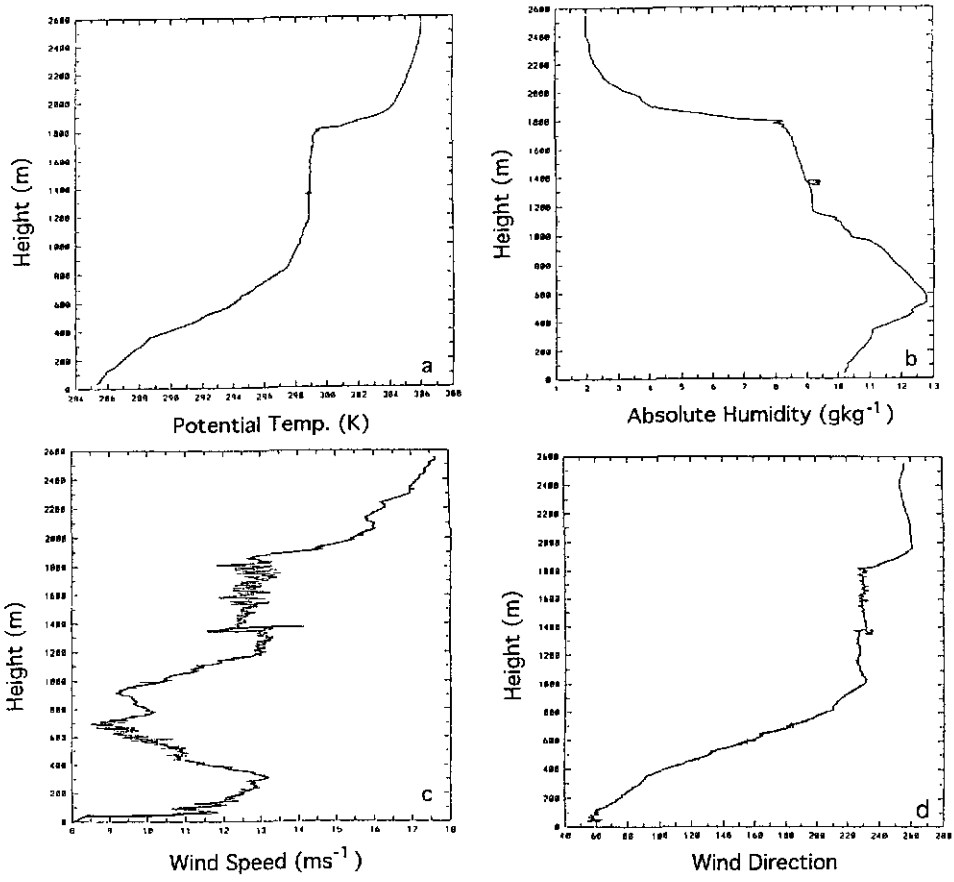

Figure 13. Vertical profiles of (a) potential temperature (K), (b) absolute humidity (g kg^{-1}), (c) wind speed (m s^{-1}), and (d) wind direction. These profiles were obtained by the King Air aircraft over cold shelf waters on 22 February 1986.

continental air. Winds near the surface were northeasterly (up to 150 m) veering almost linearly with height to southwesterly at 1200 m, indicating that the coastal front was located further offshore. Figure 13b shows the humidity profile at B. A cloud layer was present up to 600 m. Absolute humidity increased from the surface to 600 m within the coastal front and decreased in the neutral layer, as expected. The wind speed profile (Figure 13c) indicates a strong low-level jet (LLJ) at 300 m with a maximum speed of 13.5 m s^{-1}. The profile for wind direction (Figure 13d) indicated large directional shear within the front. In the lowest 200 m, the mean flow was northeasterly (onshore).

Figure 14 shows the vertical profiles of wind speeds at various locations along the east coast (HAT, ILM, MYR and CHS, see Figure 1 for location) and over the warm Gulf Stream waters (RVC, see Figure 1 for location) at 1800 UTC on 22 February 1986. The winds showed a low level maximum of 8 m s^{-1} at Hatteras

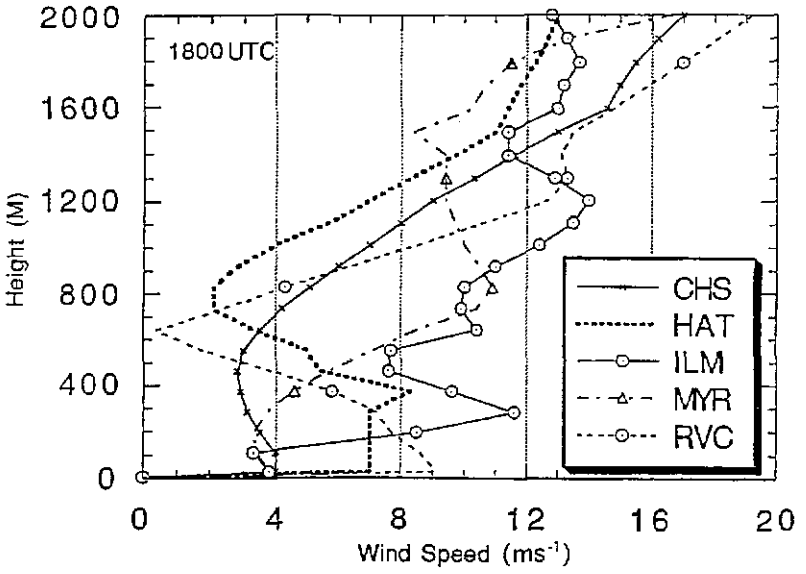

Figure 14. Vertical profiles of wind speed. Data obtained from soundings at Charleston (CHS), Cape Hatteras (HAT), Wilmington (ILM), Myrtle Beach (MYR) and mobile ship RV Cape Hatteras (RVC) at 1800 UTC on 22 February. RVC was located over the warm Gulf Stream waters and the rest of the locations are along the East Coast. See Figure 1 for locations of these stations.

(HAT) and 12 m s^{-1} at Wilmington (ILM) at a height of about 300 m. These LLJs form due to the pressure gradient caused by the differences in air temperatures between the northerly flow of cold continental air over land and the warm easterly flow over the Gulf Stream (Doyle and Warner, 1990). Aircraft observations (not shown) also indicated a LLJ at 300 m with a maximum speed of 13.5 m s^{-1} just offshore of Wilmington, NC. It is apparent from Figure 14 that, south of Wilmington (MYR and CHS), the LLJ do not exist. Variations in the inversion strength may have modified the depth of the boundary-layer mixing, thereby enabling the LLJ to persist at some locations (ILM and HAT), while substantially weakening it south of Wilmington (ILM) at CHS and MYR.

9. Summary and Conclusions

Detailed mesoscale analysis of a coastal front and an offshore meso-low off the southeast coast of the United States on 22 February 1986 are presented. The analysis indicate that a meso-low developed over a Gulf Stream filament. Other embedded mesoscale features on 22 February 1986 were two convergence zones, one near the coast and the other aligned parallel to the western edge of the Gulf Stream.

Low level jets (LLJs) were present at several locations along the coast, at Wilmington, Cape Hatteras and over the coastal shelf waters. LLJs were not observed

at locations south of Wilmington, NC such as Myrtle Beach (MYR) and Charleston (CHS).

Estimation of the frontogenesis terms at 1800 UTC on 22 February 1986 indicated the dominance of the diabatic heating term as compared to the confluence term. The confluence term was significant only along the existing confluent axes. The diabatic term was dominant in the vicinity of the surface frontal zone. However, both the terms combined together had significant influence on the formation of the coastal front.

Acknowledgements

Authors wish to thank Dr. A.J. Riordan for several helpful suggestions. This study was supported by the Division of Atmospheric Sciences, National Science Foundation under grant ATM-92-12636 and by the Naval Research Laboratory. Computational resources were provided by the North Carolina Super Computing Center, Research Triangle Park.

References

Ballentine, R. J.: 1980, 'A Numerical Investigation of New England Coastal Frontogenesis', *Mon. Wea. Rev.* **108**, 1479–1497.

Bosart, L. F., Vaudo, C. J., and Helsdon, Jr., J. H.: 1972, 'Coastal Frontogenesis', *J. Appl. Meteorol.* **11**, 1236–1258.

Bosart, L. F.: 1975, 'New England Coastal Frontogenesis', *Quart. J. Roy. Meteorol. Soc.* **101**, 957–978.

Bosart, L. F. and Lin, S. C.: 1984, 'A Diagnostic Analysis of the Presidents' Day Storm of February 1979', *Mon. Wea. Rev.* **112**, 2148–2177.

Brown, E. N., Friehe C. A., and Lenschow, D. H.: 1983, 'The Use of Pressure Fluctuations on the Nose of an Aircraft for Measuring Air Motion', *J. Clim. Appl. Meteorol.* **22**, 171–180.

Dirks, R. A., Kuettner, J. P., and Moore, J. A.: 1988, 'Genesis of Atlantic Lows Experiment (GALE): An Overview', *Bull. Amer. Meteor. Soc.* **69**, 148–160.

Doyle, J. D. and Warner, T. T.: 1990, 'Mesoscale Coastal Processes during GALE IOP 2', *Mon. Wea. Rev.* **118**, 283–308.

Doyle, J. D. and Warner, T. T.: 1993, 'A Numerical Investigation of a Coastal Frontogenesis and Mesoscale Cyclogenesis During GALE IOP 2', *Mon. Wea. Rev.* **121**, 1048–1077.

Holt, T. and Raman, S.: 1990, 'Marine Boundary Layer Structure and Circulation in the Region of Offshore Redevelopment of a Cyclone During GALE', *Mon. Wea. Rev.* **118**, 382–410.

Holt, T. and Raman, S.: 1992, 'Three Dimensional Mean and Turbulence Structure of a Coastal Front Influenced by the Gulf Stream', *Mon. Wea. Rev.* **120**, 17–39.

Hsu, S. A.: 1984, 'Sea-Breeze Like Winds Across the North Wall of the Gulf Stream: An Analytical Model', *J. Geophys. Res.* **89**, 2025–2028.

Huang, C. Y. and Raman, S.: 1990, 'Numerical Simulations of Cold Air Advection Over the Appalachian Mountains and the Gulf Stream', *Mon. Wea. Rev.* **118**, 343–362.

Huang, C. Y. and Raman, S.: 1992, 'A Three Dimensional Numerical Investigation of Carolina Coastal Front and the Gulf Stream Rainband', *J. Atmos. Sci.* **49**, 560–584.

LeMone, M. A. and Pennell, W. T.: 1980, 'A Comparison of Turbulence Measurements from Aircraft', *J. Appl. Meteorol.* **19**, 1420–1437.

Lenschow, D. H. and Spyers-Duran, P.: 1986, 'Measurement Techniques: Air Motion Sensing', *NCAR Bull. No.* **23**. [Available from NCAR, Boulder, CO 80307.]

Lind, R. J. and Shaw, W. J.: 1990, 'The Time-Varying Calibration of an Airborne Lyman-α Hygrometer', *J. Atmos. Oceanic Technol.* **8**, 186–190.

Mercer, T. J. and Kreitzberg, C. W.: 1986, *GALE Field Program Summary*, Dept. of Physics and Atmospheric Sciences, Drexel University, Philadelphia, PA 19104.

Nielsen, J. W.: 1989, 'The Formation of New England Coastal Fronts', *Mon. Wea. Rev.* **117**, 1380–1401.

Raman, S. and Riordan, A.: 1988, 'The Genesis of Atlantic Lows Experiment: Planetary Boundary Layer Subprogram of GALE', *Bull. Amer. Meteorol. Soc.* **69**, 161–172.

Reddy, N. C. and Raman, S.: 1994, 'Observations of a Mesoscale Circulation Over the Gulf Stream Region', *The Glo. Atmos. and Ocean Sys.* **2**, 21–39.

Richwein, B. A.: 1980, 'The Damming Effect of the Southern Appalachians', *Nat. Wea. Dig.* **5**, 2–12.

Riordan, A. J.: 1990, 'Examination of the Mesoscale Features of the GALE Coastal Front of 24–25 January 1986', *Mon. Wea. Rev.* **118**, 258–282.